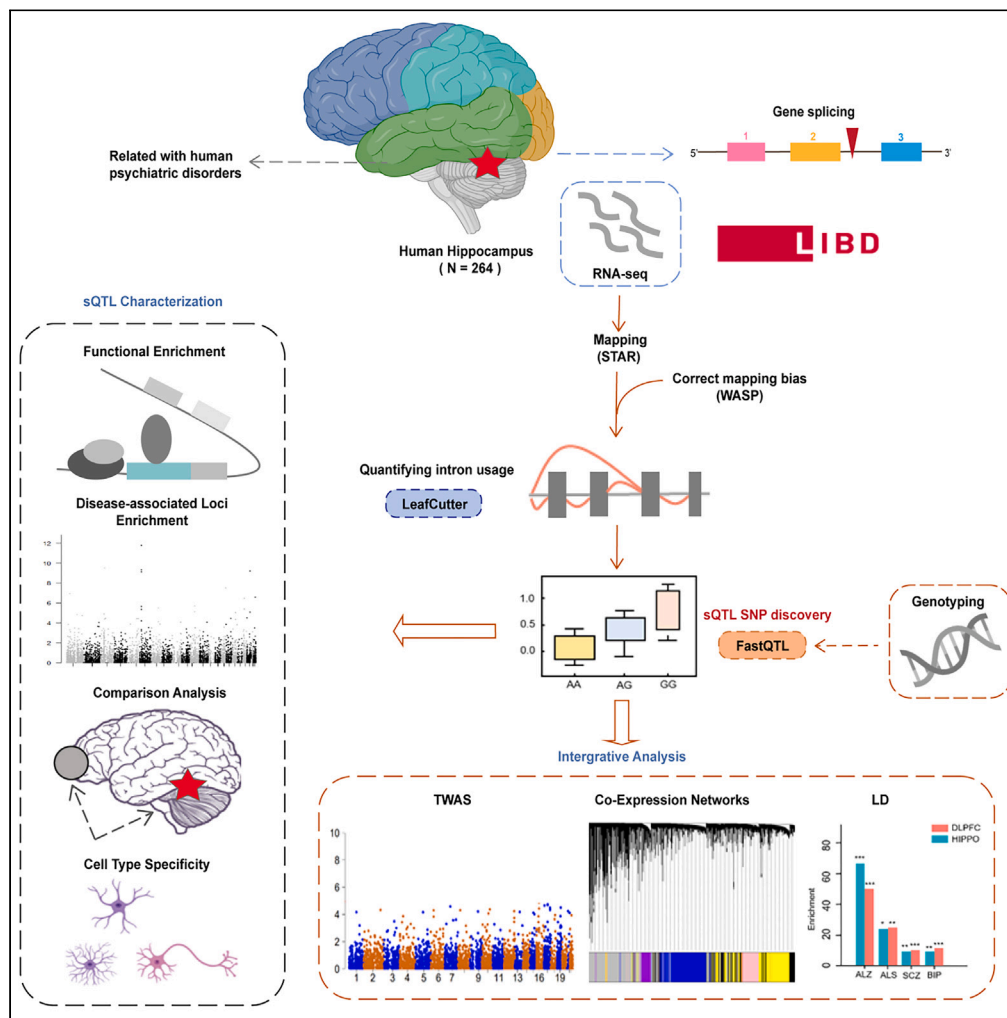


Article

Identification of region-specific splicing QTLs in human hippocampal tissue and its distinctive role in brain disorders



Xiaoyan Li, Yiran Zhao, Hui Kong, Chengcheng Song, Jie Liu, Junfeng Xia

jfxia@ahu.edu.cn

Highlights

The most comprehensive sQTL map of HIPPO was obtained by sQTL detection

We decoded these sQTL SNPs function characteristics and function enrichment

TWAS identified 16 significant genes associated with Alzheimer at the splicing level

Our work offers new hope for understanding how AS regulation contributes to brain disease



Article

Identification of region-specific splicing QTLs in human hippocampal tissue and its distinctive role in brain disorders

Xiaoyan Li,^{1,2} Yiran Zhao,^{1,2} Hui Kong,¹ Chengcheng Song,¹ Jie Liu,¹ and Junfeng Xia^{1,3,*}

SUMMARY

Alternative splicing (AS) regulation has an essential role in complex diseases. However, the AS profiles in the hippocampal (HIPPO) region of human brain are underexplored. Here, we investigated *cis*-acting sQTLs of HIPPO region in 264 samples and identified thousands of significant sQTLs. By enrichment analysis and functional characterization of these sQTLs, we found that the HIPPO sQTLs were enriched among histone-marked regions, transcription factors binding sites, RNA binding proteins sites, and brain disorders-associated loci. Comparative analyses with the dorsolateral prefrontal cortex revealed the importance of AS regulation in HIPPO ($r_g = 0.87$). Furthermore, we performed a transcriptome-wide association study of Alzheimer's disease and identified 16 significant genes whose genetically regulated splicing levels may have a causal role in Alzheimer. Overall, our study improves our knowledge of the transcriptome gene regulation in the HIPPO region and provides novel insights into elucidating the pathogenesis of potential genes associated with brain disorders.

INTRODUCTION

Alternative splicing (AS) is an essential post-transcriptional regulatory process that enhances the diversity and complexity at the RNA level through intron excision and exon ligation.^{1,2} By alternative pre-mRNA splicing, multiple transcripts, and protein isoforms can be generated from a single gene with different biological functions.³ Emerging as one of the most important mechanisms regulating gene expression, AS events affects about 95% of human multi-exon genes,⁴ which often occur in a cell or tissue-type specific manner.⁵ Notably, the molecular mechanism of AS is particularly prevalent and intricate in the human brain,⁶ suggesting that such highly complex AS regulation in brain tissue can play a crucial role in the normal development and functional maintenance of the central nervous system.^{7,8} Furthermore, accumulating studies have indicated that aberrant splicing of a specific gene affected by genetic variants may be involved in the etiology and pathogenesis of various brain disorders.^{9,10} For instance, Xu et al. found that multiple *de novo* gene mutations with strong genetic evidence can confer the risk of schizophrenia by affecting AS.¹¹ Multiple human postmortem brain studies have also reported AS dysregulation among individuals with Alzheimer's disease,^{12,13} Parkinson disease,¹⁴ and autism spectrum disorders.^{15,16}

Recent large-scale transcriptome analyses have identified thousands of genetic variants throughout the genome that play a regulatory role in AS, referred to as splicing quantitative trait loci (sQTL).⁹ Therefore, sQTL analysis is conducted to gain greater insight into the associations between genetic variants and AS regulation.¹⁷ The splicing level of a splice site or alternative exon can be considered as quantitative traits and maps to a genomic variant within a population in sQTL analysis. Previous studies have indicated that sQTLs have similar or even greater effects on diseases and complex traits compared to expression quantitative trait loci (i.e., eQTL, meaning genetic variants affecting gene expression), highlighting the utility of sQTLs as a crucial approach for uncovering genetic variants of AS regulation.⁹ Through sQTL analysis, several recent studies have successfully explored how functional genetic variation impacts AS (i.e., the splicing level) in human.^{18,19} However, there are relatively few sQTL analyses based on RNA sequencing (RNA-seq) of the brain^{20–22} (i.e., most of these analyses mainly focused on non-neuronal tissues), and none include a comprehensive sQTL analyses of the postmortem hippocampal (HIPPO) brain tissue.

Mounting evidence suggests that HIPPO region damage prominently implicated in the etiology and pathogenesis of brain disorders, including schizophrenia, Alzheimer, epilepsy, depression and anxiety, but there is less research accessible since current large consortia favor research on neocortical brain regions like the dorsolateral prefrontal cortex (DLPFC).^{23,24} Here, to comprehensively investigate sQTLs in the HIPPO region of the human brain, we utilized transcriptome data and genotype data from 264 individuals in the second phase of the BrainSeq Consortium (i.e., BrainSeq2²⁵). We eventually identified a total of 6,966 sQTLs involving in 14,559 AS events of 5,299 unique genes (defined as sGenes) that are expected to be independent of one another after undergoing stringent quality control. The functional characterization of

¹Information Materials and Intelligent Sensing Laboratory of Anhui Province and Key Laboratory of Intelligent Computing and Signal Processing of Ministry of Education, Institutes of Physical Science and Information Technology, Anhui University, Hefei, Anhui 230601, China

²These authors contributed equally

³Lead contact

*Correspondence: jfxia@ahu.edu.cn

<https://doi.org/10.1016/j.isci.2023.107958>



these sQTL single nucleotide polymorphisms (SNPs) was examined, and we comprehensively described the implicated regulatory regions associated with sQTL variants as well as the genetic contribution of sQTL variants to the etiology of brain disorders. By comparing sQTL signals between HIPPO and DLPFC brain regions, we found a large genetic similarity between the two brain regions ($r_g = 0.87$, calculated by ldsc). In addition, transcriptome-wide association studies (TWAS) integrating sQTLs summary data and genetic association signals from the genome-wide association studies (GWASs) of Alzheimer's disease have been performed to unravel novel susceptibility genes in HIPPO tissue. In conclusion, these findings provide a comprehensive sQTLs map in the HIPPO brain, which can advance our understanding of the genetic architecture of complex brain disorders.

RESULTS

Robust identification of *cis*-sQTLs in human HIPPO region

Genetic variants with effects on RNA splicing are an important factor contributing to brain diseases risk. Considering that splicing regulation in the HIPPO region of the human brain has not been systematically explored, we performed a sQTL analysis of the HIPPO region to enhance the understanding of the link between splicing and brain diseases. All individuals ($N = 264$) from BrainSeq2 with no history of neurological and/or neuropsychiatric diseases were included in the sQTL analysis. We first employed LeafCutter to analyze RNA-seq data to comprehensively identify AS events in human HIPPO region. The regulation of brain splicing generates a large number of homologous genes, leading to incomplete isoform annotations in brain. LeafCutter is an annotation-free method that allows for alternative exon identification and therefore has important advantages in the context of brain. We then conducted *cis*-sQTLs (*cis*-window of ± 100 kb around the AS event) discovery using the linear regression model implemented in FastQTL. After applying stringent quality control and normalization (see STAR methods for details), we obtained a total of 11,157 significant sQTLs ($FDR < 0.05$) involving in 16,492 AS events of 6,387 unique genes (Table S1). Positional enrichment of sQTL SNPs showed that most of significant sQTL SNPs (i.e., with strong effects on splicing) were mainly enriched in exons or proximal introns regions (± 100 bp of junction) (Figure 1A). This observation is consistent with prior findings^{26,27} that many variants within these regions have an impact on AS regulatory functions, indicating that sQTL SNPs closer to their splice sites had a significant effect on AS.

Functional characterization of sQTL SNPs

To characterize the function of each sQTL SNPs, we generated sQTL and non-sQTL datasets for comparative analysis. After sQTL SNPs extracting (p-value filtering) and LD pruning (see STAR methods), we obtained sQTL and non-sQTL SNPs dataset, containing 6,966 SNPs (contributed to AS regulation independently) and 124,801 SNPs (not contributed to AS regulation independently), respectively. We first functionally classified these sQTL (Table S3A) and non-sQTL SNPs (Table S3B) with the variant types defined by SnpEff (Figure 1B). As expected, we found that the sQTL SNPs were significantly enriched in exonic regions (correspond to red in Figure 1B) compared to non-sQTL SNPs ($p = 2.43 \times 10^{-76}$, odds ratio (OR) = 2.13, two-tail Fisher's exact test). We then performed functional enrichment of sQTL SNPs among different variant types. Notably, the enrichment of variants located in the splice region was the most significant compared to non-QTL SNPs ($p = 8.65 \times 10^{-62}$, OR = 4.83, two-tail Fisher's exact test), suggesting that splice site variants may plays an important role in AS regulation (Figure 1C). Moreover, there was significant enrichment of splice acceptor ($p = 3.48 \times 10^{-18}$, OR = 17.94, two-tail Fisher's exact test) and splice donor ($p = 2.86 \times 10^{-15}$, OR = 14.23, two-tail Fisher's exact test), and underrepresentation of intergenic variants (Figure 1C).

Functional enrichment of sQTLs SNPs in regulatory elements and RBP binding sites

Previous studies have shown that regulatory elements (H3K4me1, H3K4me3, H3K9ac, H3K27ac, and DHS) and RBPs facilitate AS regulation during transcription,^{18,21} so we explored whether genomic regions tagged by sQTL SNPs are enriched in regulatory elements and RBP binding sites to understand the mechanism by which sQTL SNPs influence AS regulation (see STAR methods section for details). For regulatory elements, we found that sQTL SNPs are significant enriched in H3K4me3 ($p = 2.04 \times 10^{-21}$, OR = 2.10, two-tail Fisher's exact test with), H3K9ac ($p = 1.69 \times 10^{-17}$, OR = 1.89, two-tail Fisher's exact test with) and H3K27ac ($p = 1.19 \times 10^{-18}$, OR = 1.91, two-tail Fisher's exact test markers compared to non-sQTL SNPs (Figure 2A). Increasing evidence indicates that H3K4me3 marks plays an important role in AS regulation.²⁸⁻³⁰ It was previously reported that H3K4me3 histone modification was involved in AS regulation through control of spliceosome recruitment.²⁹ According to the scoring criteria defined by RegulomeDB (Table S4), we found that sQTL SNPs were significantly enriched in SNPs with in the category with a score of one (i.e., these SNPs have been experimentally shown to affect TFs binding) compared to non-sQTL SNPs ($p = 1.32 \times 10^{-42}$, OR = 2.51, two-tail Fisher's exact test), indicating that these TFs affected by sQTL SNPs plays an important role in AS regulation (Figure 2B). For RBP binding sites, as expected, we observed that sQTL SNPs were significantly enriched in 30 RBPs binding sites (Figure 2C), providing further evidence that these sQTL SNPs fall in RBPs binding sites relevant to the AS regulation. Notably, identified RBPs with prominent known roles in brain RBPs include *SRSF1*,³¹ *LIN28B*,³² *TARDBP*,³³ *ELAVL1*,³⁴ *DDX3X*,³⁵ and *ATXN2*,³⁶ while the functional significance of the remaining RBPs is unclear.

Enrichment analysis of sQTL SNPs among brain disease-associated loci

To identify the potential contribution of sQTL SNPs to the risk of brain-related diseases, we utilized data mined from the GWAS catalog to perform enrichment analysis for identified sQTL and non-sQTL SNPs. By exploring whether sQTL SNPs are significantly enriched for GWAS loci associated with 12 brain disorders (see STAR methods), we found the sQTL SNPs were significantly enriched in brain disorders compared to non-sQTL SNPs ($p < 1.00 \times 10^{-3}$, OR = 4.84, one-tailed Fisher's exact test). Enrichment analysis of sQTL SNPs using summary data from the

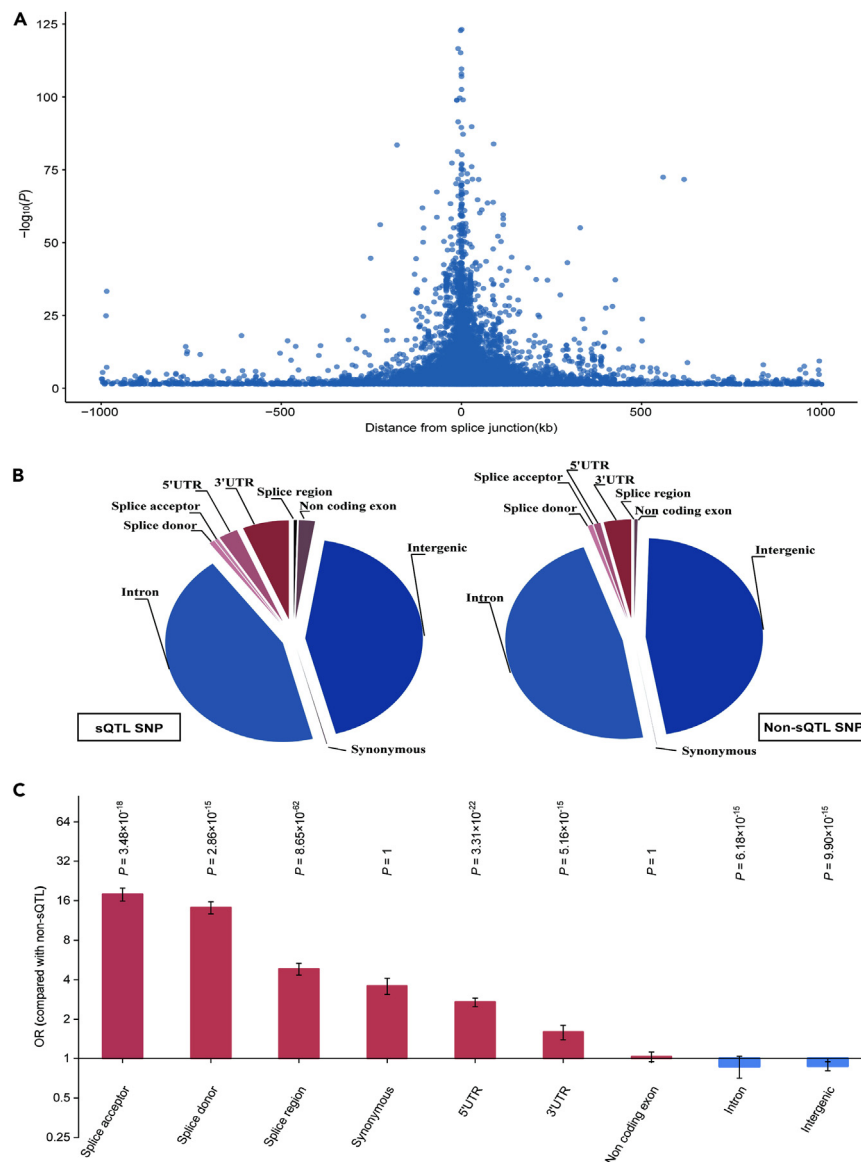


Figure 1. Characterization of identified sQTL SNPs

(A) Each blue dot represents an SNP plotted according to its distance from the nearest AS event and the statistical significance of its association with AS ($-\log_{10}$ p-value).

(B) Pie charts indicating proportions of SNPs annotated with each functional category (splice acceptor, splice donor, splice region, synonymous, 5' UTR, 3' UTR, non-coding exon, intron and intergenic). SNPs in exonic regions (nonsense, readthrough, start-loss, frameshift, canonical splice site, missense, synonymous, splice region, 5' UTR, 3' UTR and non-coding exon) and SNPs in non-exonic regions (intron and intergenic) are indicated by red and blue colors, respectively.

(C) Enrichment of sQTL SNPs in each different functional type of variants. Exonic variants are shown in red and non-exonic variants are shown in blue. p-values were calculated by two-tailed Fisher's exact test with Bonferroni correction. Bars indicate 95% confidence intervals.

largest GWAS to date for individual brain disorders was further performed. The most significant enrichment among psychiatric disorders was observed for schizophrenia ($p = 2.06 \times 10^{-47}$, OR = 4.36), and the most significant enrichment among neurodegenerative disease was observed for Alzheimer ($p = 6.48 \times 10^{-53}$, OR = 7.05) (Figure 2D). These results suggested that some of these SNPs probably contribute to disease (including schizophrenia and Alzheimer) risk by affecting AS.

Enrichment of sGenes in different cell types of the brain

To further identify the cell types associated with AS regulation, EWCE was used to estimate the enrichment of these identified sGenes to various cell types. We found that sGene was significantly (Benjamini-Hochberg $p < 0.05$) enriched in a variety of cell types, including astrocytes

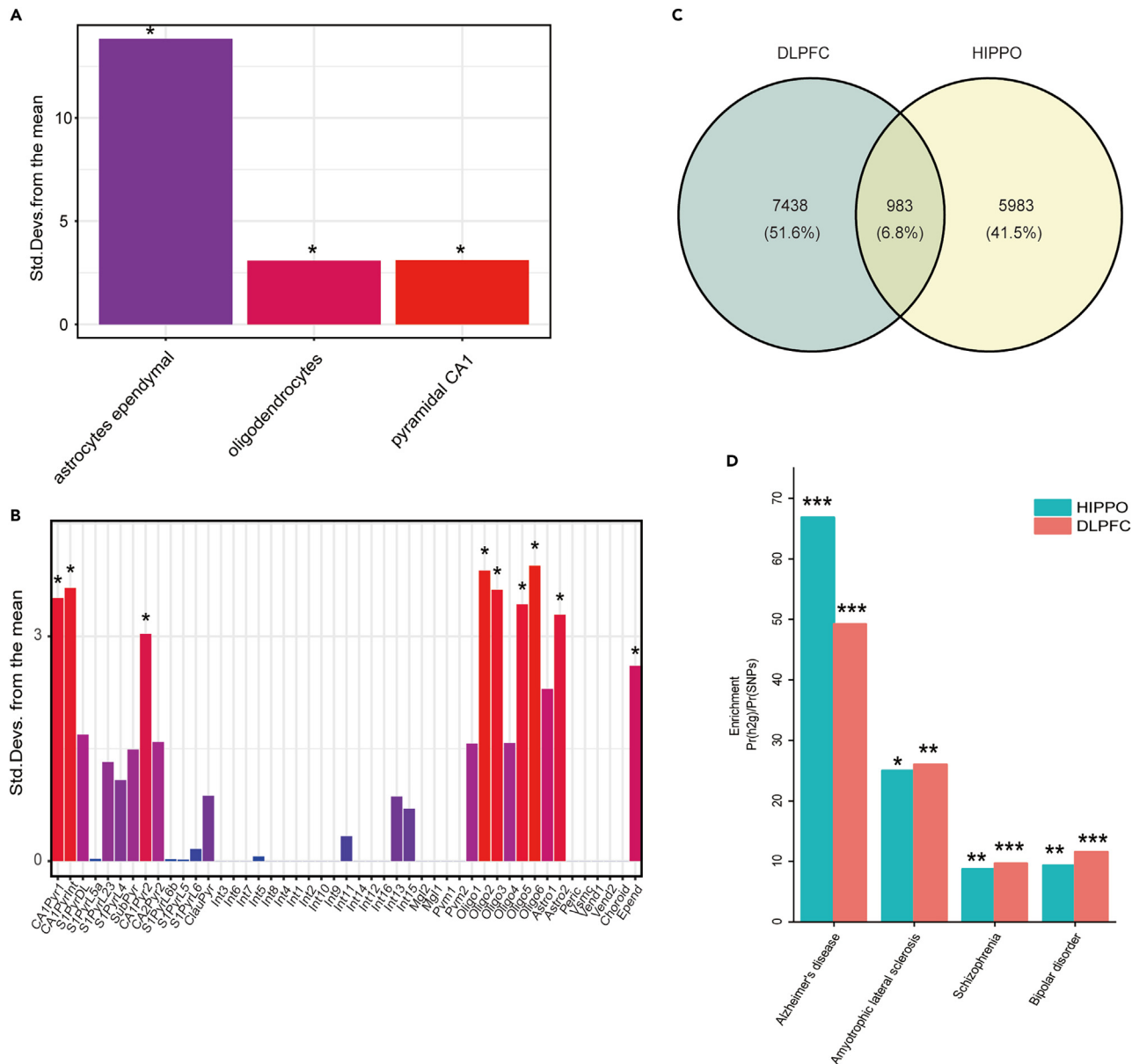


Figure 3. Enrichment of sGenes in different cell types of the brain and their comparison to DLPFC sQTLs

(A) Associations between sGenes and cell types from somatosensory cortex and hippocampal CA1 in mice were marked with asterisks, indicating Benjamini-Hochberg significance ($p < 0.05$). The results show 3 significantly enriched cell types in the primary classification ($p < 0.05$), including astrocytes oligodendrocytes and pyramidal CA1.

(B) The results show 9 significantly enriched cell types in the secondary classification ($p < 0.05$).

(C) The Venn diagram shows the number and percentage of sQTL SNPs that overlap in the two brain regions.

(D) Partitioning heritability enrichment of four brain disorders (Alzheimer's disease, amyotrophic lateral sclerosis, schizophrenia, and bipolar disorder) in two brain regions, $p < 0.05$ was significant (Bonferroni-Corrected-value threshold). Among the four diseases, Alzheimer's disease was the most significantly enriched, especially in the HIPPO. One asterisk (*) indicates a p -value < 0.05 ; two asterisk (**) indicate a p -value < 0.01 , and three asterisk (***) indicate a p -value < 0.001 .

and endothelial cell. Interestingly, we observed that sGenes were significantly enriched in AST1, AST2, AST3, AST4, AST5, and oligodendrocyte cell types in both HIPPO and cortex regions. (Figure S2). Many studies have reported the association of astrocytes with diseases, including Alzheimer's disease.^{37,38} For example, one study has reported the identification of a population of disease-associated astrocytes in a mouse model of Alzheimer's disease,³⁹ suggesting that these results are consistent with our findings.

Tissue specificity of sQTLs between brain HIPPO and DLPFC regions

Previous studies have showed that AS events associated with brain diseases tend to be brain region-specific,²² indicating that there are differences between HIPPO and DLPFC region sQTLs at the level of SNPs. By performing the same sQTL mapping analysis on the DLPFC region (the specific procedure is the same as HIPPO, see [STAR methods](#) section for details), we observed approximately 6.8% of sQTL SNPs overlapped between the HIPPO and DLPFC (as shown in the [Figure 3C](#)), and we noted that the p values of the overlapping sQTL SNPs were highly significant in both brain regions. To further measure the genetic similarity of sQTLs in two different brain regions, we calculated r_g using the *ldsc* software⁴⁰ ($r_g = 0.87$), indicating a strong genetic similarity between the two brain regions. We further compared the enrichment patterns of 12 brain disease-associated GWAS in sQTL from HIPPO brain regions and DLPFC brain regions, and found significant enrichment in four brain disorders ([Figure 3D](#)). Among them, Alzheimer-associated variants are the most significantly enriched in the HIPPO and DLPFC regions ($p = 9.49 \times 10^{-6}$ and $p = 8.15 \times 10^{-4}$, respectively) ([Figure 3D](#)). Interestingly, sQTL SNPs showed more significant enrichment in HIPPO brain regions compared to DLPFC, suggesting that Alzheimer-related risk variants may be more relevant to HIPPO brain regions. Therefore, studying AS events in HIPPO brain regions for Alzheimer deserves in-depth study. Additionally, genetic variants associated with risk for amyotrophic lateral sclerosis ($p = 2.28 \times 10^{-2}$ and $p = 5.73 \times 10^{-3}$, respectively), schizophrenia ($p = 1.45 \times 10^{-3}$ and $p = 1.76 \times 10^{-4}$, respectively) and bipolar disorder ($p = 1.22 \times 10^{-3}$ and $p = 1.10 \times 10^{-4}$, respectively) were significantly enriched for both HIPPO and DLPFC regions, whereas depression GWAS was not significant for both regions ([Figure 3D](#)). Overall, these results are consistent with previous findings⁴¹ that sQTL SNPs identified by HIPPO harbor substantial disease risk, suggesting AS regulation in the HIPPO brain region deserves further study in brain disorders development.

sGenes with the context of splicing networks

By constructing a splicing co-expression network using robust WGCNA, we identified a total of 14 functional modules of co-expressed sGenes in the HIPPO region ([Figure 4A](#)). We performed GO and KEGG enrichment analysis of obtained sGenes modules to identify important biological processes and metabolic pathways ([Table S5A](#)). One interesting splicing co-expressed module are turquoise module with the highest number of sGenes ([Figure 4B](#)), which was enriched for regulation of mRNA metabolic and RNA splicing process ([Figure 4C](#)). Specifically, GO analysis showed that the sGenes contained in the turquoise module were mainly enriched in splicing- and neurodevelopment-associated pathways, including RNA splicing, regulation of RNA splicing, modulation of chemical synaptic transmission, regulation of *trans*-synaptic signaling, axonal transport, axo-dendritic transport ([Figure 4D](#); [Table S5B](#)). KEGG analysis showed that the sGenes contained in the turquoise module were mainly enriched in the pathways related to spliceosome and dopaminergic synapse ([Figure 4E](#); [Table S5B](#)), suggesting that the sGenes have an important function in the AS regulation and synaptic transmission.

TWAS prioritize potential causal genes for Alzheimer

The most significant enrichment among Alzheimer-associated loci observed above ([Figure 2D](#)) suggested that some of these SNPs could confer risk for Alzheimer's disease by affecting AS. To further leverage these sQTLs data (using intron excision levels as a reference panel) identified in HIPPO to prioritize potential causal genes for Alzheimer, we performed a TWAS incorporating *cis*-sQTLs and Alzheimer GWAS. After Bonferroni correction, we identified 16 genes with intron associations whose imputed *cis*-regulated expression is associated with Alzheimer ([Figure 5A](#)) ([Table S6](#)). Of note, *APOC1* showed the most significant association, strongly suggesting that *APOC1* is a promising causal gene for Alzheimer. Our sQTL analysis showed that rs56131196 was associated with the splicing levels of *APOC1* ($P_{\text{corrected}} = 1.56 \times 10^{-3}$) (i.e., differential intronic usage for chr19:45419582:45434257 stratified by rs56131196 genotypes) ([Figure 5B](#)), suggesting that *APOC1* could causally confer Alzheimer risk by affecting AS in the human HIPPO brain. Other top significant genes include *PVR*, *ZNF138*, *ERCC1*, *CD2AP*, *KNSTRN*, *ANK3*, *STAG3*, *CRYL1*, *SLC12A9*, *SNRPC*, *HMGCLL1*, *LAMTOR4*, *CCDC18*, *SLC39A13*, and *PTK2B*. These significant genes represent promising candidate causal genes for Alzheimer. To identify novel risk regions beyond the Alzheimer GWAS identification, we then examined the overlap between the 38 independent genome-wide significant Alzheimer GWAS loci and significant HIPPO TWAS associations. We observed seven GWAS loci harbor HIPPO TWAS associations (overlap of TWAS significant loci (± 500 kb) with GWAS significant loci), and nine additional Alzheimer risk loci where significant TWAS loci do not overlap GWAS significant loci. Given the evidence that the HIPPO is associated with the development of Alzheimer's disease, we believed that these HIPPO sQTLs data would provide new perspectives on Alzheimer risk, especially given the sensitivity of AS regulation to tissue source.

DISCUSSION

Our work provides the most comprehensive genome-wide sQTLs map of the HIPPO, a critical region in brain prominently implicated in the pathogenesis of brain disorders, significantly expanding our understanding of AS regulation in the HIPPO brain. We have comprehensively characterized properties and regulatory elements of the detected sQTL SNPs, enabling the incorporation of tissue specificity to previous brain genetic variant interpretation and functional genomic analysis. By comparing sQTLs of the HIPPO and DLPFC region from the same individuals, we found that approximately over 90% of significant sQTLs in HIPPO are distinct from DLPFC, indicating that sQTL detecting in HIPPO warrants more attention in future studies. By integrating sQTLs with GWAS data via TWAS, we identified novel putative mechanisms detected in HIPPO brain datasets, demonstrating the distinct contribution of sQTLs to the genetic architecture underpinning brain disorders

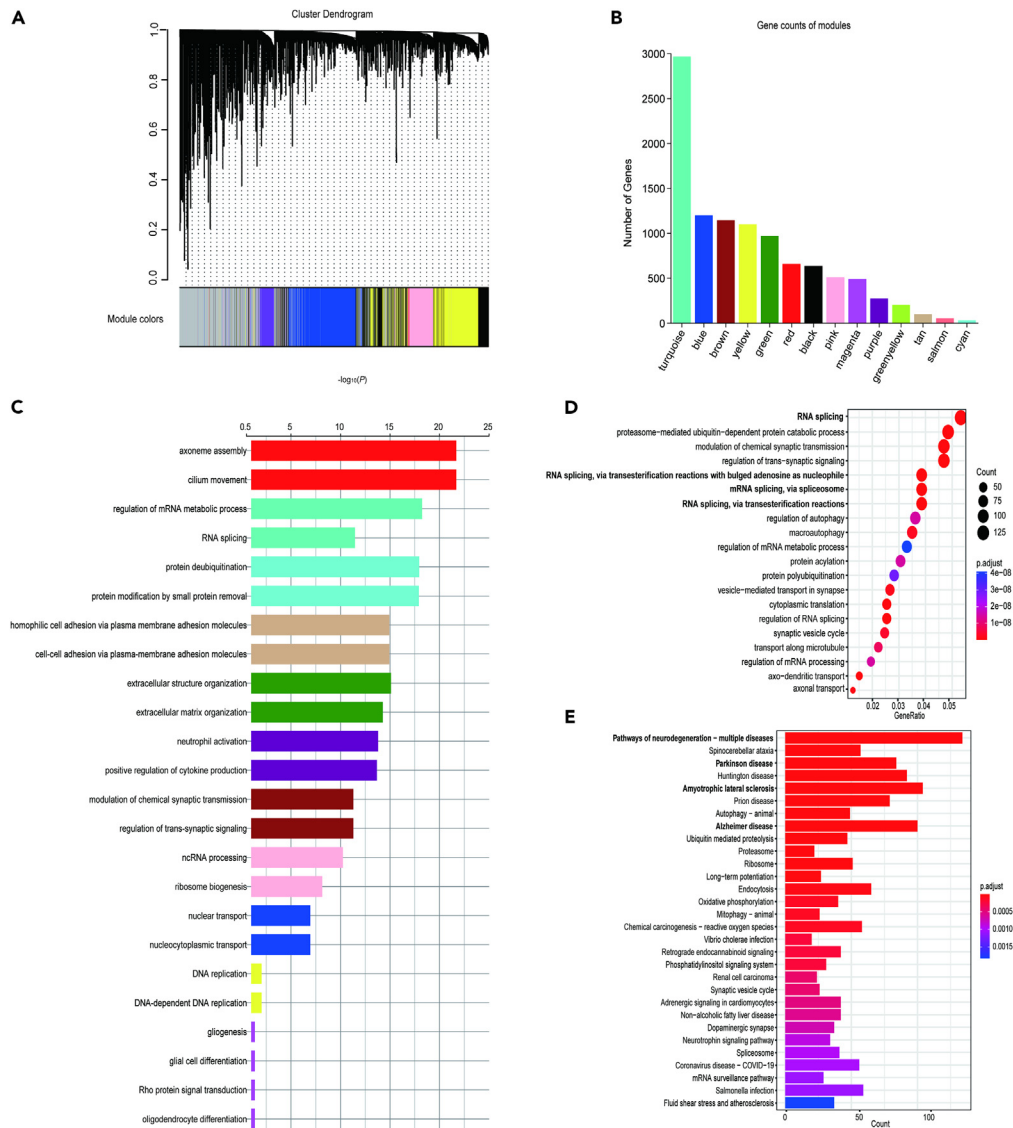


Figure 4. Splicing co-expression networks in HIPPO

(A and B) (A) Network analysis dendrogram based on hierarchical clustering of sGenes by their topological overlap, identifies 14 modules, and (B) indicates the number of differential sGenes enriched in each module, with the most enriched sGenes in the turquoise module.

(C–E) (C) GO analysis was performed on the sGenes of each module, and the first two most significant results were extracted (The p-value was corrected by Benjamini-Hochberg). The turquoise cluster module is involved in RNA-splicing processes and various neurodegenerative disease pathways as described in detail by (D) GO and (E) KEGG analyses.

variation. These results collectively confirmed that sQTL SNPs identified in the HIPPO is a key data resource for deciphering the genetic mechanisms underlying complex brain disorders.

To further leverage these splicing to characterize Alzheimer loci with the specific brain region, we performed a TWAS analysis by integrating *cis*-sQTLs and GWAS to identify potential risk genes whose change in splicing are associated with Alzheimer. Our analysis corroborated seven known Alzheimer genes, including *APOC1*,⁴² *STAG3*,⁴³ *CRYL1*,⁴⁴ *SNRPC*,⁴⁵ *LAMTOR4*,⁴⁶ *SLC39A13*,⁴⁷ and *PTK2B*,⁴⁸ and also identified nine genes that have not previously been reported in suggestive Alzheimer loci. As a proof of principle, we highlight two of these genes: *ERCC1* and *ANK3*. *ERCC1* is a protein coding gene, which is involved⁴⁵ in the recognition and nucleotide excision repair pathway.⁴⁹ Interestingly, age-related motor neuron degeneration has been observed in *Erc1* (*Delta*^{-/-}) mice with impaired DNA repair systems.⁵⁰ Considering that Alzheimer’s disease is the most important age-related neurodegenerative disorder, these results demonstrate that *ERCC1* may confer risk of Alzheimer by affecting the function of age-related motor neurons. *ANK3* (ankyrin 3, node of Ranvier) encodes ankyrin 3 or G, which functions as a scaffold linking plasma membrane proteins to the actin/ β -spectrin cytoskeleton.⁵¹ Notably, *ANK3* has been reported

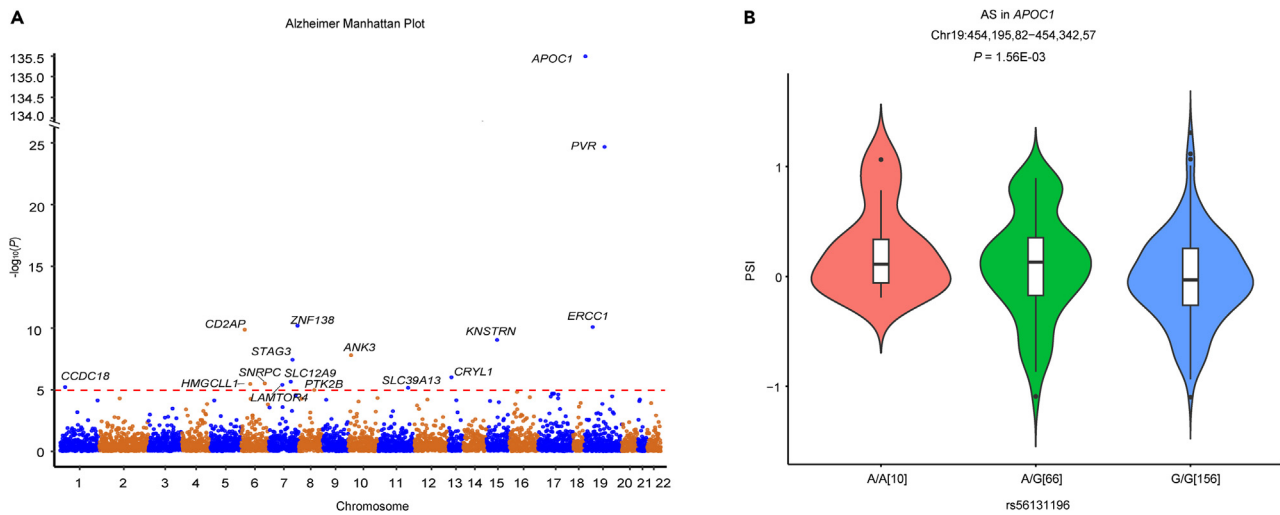


Figure 5. TWAS in Alzheimer's disease

(A) Manhattan plot of TWAS results from intron Alzheimer associations, highlighting the 16 significant gene. The red solid line represents Bonferroni corrected p-value threshold (i.e., $p = 1.13 \times 10^{-5}$).

(B) The violin diagram shows association of rs56131196 with the PSI of *APOC1* in our dataset ($P_{corrected} = 1.56 \times 10^{-3}$ in our sQTL analysis). The distribution of PSI abundances in a genotype class, that is, AA (N = 10), AG (N = 66), or GG (N = 156). The superimposed boxplot is shown with horizontal black lines and white boxes for median and quartile distances, respectively. Outliers are shown as black dots.

to contribute significantly in the brain specific isoforms found in axons, particularly associated with the voltage-dependent sodium channel.⁵² Evidence from linkage studies suggests that *ANK3* are involved in the genetic architecture of late-onset Alzheimer's disease,⁵³ indicating that this gene is a particularly promising candidate for Alzheimer locus. Therefore, our results provide further support and guidance for future experimental validation and serve to elucidate the role of these sQTL SNPs in the etiology of Alzheimer.

We also explored the potential function of allele-specific sQTL for gene *ApoE4* or other key susceptible genes of Alzheimer summarized by Pasqualetti G et al.'s work.⁴⁸ For gene *ApoE4*, we found that *ApoE4* were not identified in our HIPPO sQTL analysis, possibly due to the use of normal human rather than Alzheimer patient samples for sQTL analysis and sample size limitations. For other key susceptible genes (N = 32) of Alzheimer, we found that several SNPs were significantly associated with the splicing levels of *ZCWPW1*, *BIN1*, *CD2AP*, *CCELF1*, *HLA-DRB1*, *IQCK*, *PTK2B*, *SSLC4A4*, and *WVVOX* (Figure S3), implying that these genes could causally confer Alzheimer risk by affecting AS in the human HIPPO brain. However, we found that the remaining 23 Alzheimer key susceptibility genes were not identified in our HIPPO sQTL analysis. Obtaining genotype and transcriptome sequencing data from HIPPO brain region samples of Alzheimer patients for sQTL analysis may help to reveal the potential functions of these Alzheimer genes in the future work.

By comparing the enrichment patterns of brain disease-associated GWAS in sQTL between HIPPO and DLPFC brain regions, we found that Alzheimer-associated variants were more significantly enriched in the HIPPO regions (Figure 3D). Our results suggest that the HIPPO region may be implicated in the pathogenesis of Alzheimer's disease. Indeed, there is growing evidence that many AS events are highly brain tissue specific (i.e., highly heterogeneous).^{22,54} The DLPFC is a neocortical region that is the hub of cognitive circuits and is affected in Alzheimer. Interestingly, previous studies have reported that the HIPPO region was one of the earliest brain regions to be affected by the neuropathology of Alzheimer's disease, indicating a key role for HIPPO in Alzheimer's disease pathology.^{55,56} In addition, Alzheimer's disease is also characterized by the pathological deposition of amyloid- β peptides in the HIPPO.⁵⁷ These lines of evidence support that the HIPPO may be an important and promising brain region for Alzheimer treatment.

For regulatory elements, we found that sQTL SNPs are significant enriched in H3K4me3 ($p = 2.04 \times 10^{-21}$, OR = 2.10, two-tail Fisher's Q exact test), H3K9ac ($p = 1.69 \times 10^{-17}$, OR = 1.89, two-tail Fisher's exact test) and H3K27ac ($p = 1.19 \times 10^{-18}$, OR = 1.91, two-tail Fisher's exact test) compared to non-sQTL SNPs after performing Bonferroni correction (Figure 2A). Increasing evidence indicates that H3K4me3 marks plays an important role in AS regulation.²⁸⁻³⁰ It was previously reported that H3K4me3 histone modification was involved in AS regulation through control of spliceosome recruitment. Interestingly, we also found that sQTL SNPs were significant enriched in 5' UTRs sites (Figure 1C), implying that 5' UTRs are more prone to AS, which is consistent with results reported in the literature.⁵⁸ Growing evidence suggests that sQTL SNPs occurring at 5' UTR are involved in transcriptional activation, as the H3K4me3 marks are enriched in the 5' end of gene bodies, which normally includes the 5' UTRs.⁵⁹ In addition, the sGenes contained in the turquoise module were also enriched in brain-related disorders (Figure 4E), especially in multiple neurodegenerative diseases (including Alzheimer and Parkinson), which is consistent with the results of enrichment analyses of sQTL SNPs among disease-associated loci.

In summary, we performed a well-powered sQTL analysis in the HIPPO of human brain and further decoded these sQTL SNPs' function characteristics, regulatory elements and RBP enrichment, and associated brain disorders. Our results may advance the understanding of how functional genetic variants confer brain disease risk by affecting AS regulation in specific tissues.

Limitations of the study

Our study also has several limitations. First, although the sample size ($N = 264$) was sufficient to confidently detect sQTL in the HIPPO, most of brain disorders heritability remain unexplained. Additional significant sQTLs may be found with very large sample sizes. Second, we limited the current sQTL analysis to only tissues from a single brain region (i.e., HIPPO), which contains a mixture of multiple cell types. Since sQTLs are often occur at cell type-specific manner, this may mask the ability to detect cell-type-specific sQTLs, particularly affecting a minor cell population in the bulk tissues. Future analyses of sQTLs using large-scale RNA-seq data at cell types or single cells resolutions will provide additional informative data resource of genetically AS regulation in human brain. Third, our study identified multiple statistically significant genetic variants affecting splicing in the HIPPO, but further functional experimental validations are required to elucidate the molecular mechanisms of these significant sQTL SNPs.

STAR★METHODS

Detailed methods are provided in the online version of this paper and include the following:

- KEY RESOURCES TABLE
- RESOURCE AVAILABILITY
 - Lead contact
 - Materials availability
 - Data and code availability
- METHOD DETAILS
 - RNA-seq data of the HIPPO tissue
 - SNP genotyping data
 - Detection and quantification of AS events
 - Splicing QTL mapping
 - sQTL and non-sQTL datasets generating
 - Functional annotation of sQTL and non-sQTL SNPs
 - Functional enrichment of sQTL SNPs among genetic regulatory elements and splicing factor binding sites
 - Functional enrichment of sQTLs among brain disease-associated loci
 - DLPFC and HIPPO tissue comparison
 - Partitioned heritability
 - Expression-weighted cell type enrichment analysis (EWCE)
 - Weighted gene co-expression network analysis (WGCNA)
 - TWAS analysis
 - Multiple comparison
- QUANTIFICATION AND STATISTICAL ANALYSIS

SUPPLEMENTAL INFORMATION

Supplemental information can be found online at <https://doi.org/10.1016/j.isci.2023.107958>.

ACKNOWLEDGMENTS

We thank the participants and investigators of the BrainSeq Consortium for generating and made the summary statistics available for us and making this work possible. X.L. and J.X. acknowledge funding by the grant from the National Natural Science Foundation of China (82101611, U22A2038 and 62072003).

AUTHOR CONTRIBUTIONS

J.X. and X.L. conceived and devised this study. Y.Z. performed most of the bioinformatic analyses, including the sQTL mapping, functional enrichment analysis, WGCNA and comparative analysis. H.K. performed TWAS analysis. J.X., X.L., Y.Z., H.K., C.S., and J.L. contributed to this work in data generation, analysis, and the interpretation of the results. X.L. and Y.Z. drafted the first version in writing the manuscript. J.X. and X.L. supervised the project and were in charge of overall direction. All authors provided critical feedback and approved the final version.

DECLARATION OF INTERESTS

The authors declare that they have no competing interests.

Received: May 7, 2023

Revised: June 28, 2023

Accepted: September 14, 2023

Published: September 19, 2023

REFERENCES

- Nilsen, T.W., and Graveley, B.R. (2010). Expansion of the eukaryotic proteome by alternative splicing. *Nature* 463, 457–463. <https://doi.org/10.1038/nature08909>.
- Chen, M., and Manley, J.L. (2009). Mechanisms of alternative splicing regulation: insights from molecular and genomics approaches. *Nat. Rev. Mol. Cell Biol.* 10, 741–754. <https://doi.org/10.1038/nrm2777>.
- Islam, S., and Mukherjee, C. (2022). Molecular regulation of hypoxia through the lenses of noncoding RNAs and epitranscriptome. *Wiley Interdiscip. Rev. RNA* 14, e1750. <https://doi.org/10.1002/wrna.1750>.
- Wang, E.T., Sandberg, R., Luo, S., Khrebtkova, I., Zhang, L., Mayr, C., Kingsmore, S.F., Schroth, G.P., and Burge, C.B. (2008). Alternative isoform regulation in human tissue transcriptomes. *Nature* 456, 470–476. <https://doi.org/10.1038/nature07509>.
- Baralle, F.E., and Giudice, J. (2017). Alternative splicing as a regulator of development and tissue identity. *Nat. Rev. Mol. Cell Biol.* 18, 437–451. <https://doi.org/10.1038/nrm.2017.27>.
- Merkin, J., Russell, C., Chen, P., and Burge, C.B. (2012). Evolutionary dynamics of gene and isoform regulation in Mammalian tissues. *Science* 338, 1593–1599. <https://doi.org/10.1126/science.1228186>.
- Zhu, H., Hasman, R.A., Barron, V.A., Luo, G., and Lou, H. (2006). A nuclear function of Hu proteins as neuron-specific alternative RNA processing regulators. *Mol. Biol. Cell* 17, 5105–5114. <https://doi.org/10.1091/mbc.e06-02-0099>.
- Miura, P., Sanfilippo, P., Shenker, S., and Lai, E.C. (2014). Alternative polyadenylation in the nervous system: to what lengths will 3' UTR extensions take us? *Bioessays* 36, 766–777. <https://doi.org/10.1002/bies.201300174>.
- Li, Y.L., van de Geijn, B., Raj, A., Knowles, D.A., Petti, A.A., Golan, D., Gilad, Y., and Pritchard, J.K. (2016). RNA splicing is a primary link between genetic variation and disease. *Science* 352, 600–604. <https://doi.org/10.1126/science.aad9417>.
- Raj, B., and Blencowe, B.J. (2015). Alternative Splicing in the Mammalian Nervous System: Recent Insights into Mechanisms and Functional Roles. *Neuron* 87, 14–27. <https://doi.org/10.1016/j.neuron.2015.05.004>.
- Xu, B., Ionita-Laza, I., Roos, J.L., Boone, B., Woodruff, S., Sun, Y., Levy, S., Gogos, J.A., and Karayiorgou, M. (2012). De novo gene mutations highlight patterns of genetic and neural complexity in schizophrenia. *Nat. Genet.* 44, 1365–1369. <https://doi.org/10.1038/ng.2446>.
- Bai, B., Hales, C.M., Chen, P.C., Gozal, Y., Dammer, E.B., Fritz, J.J., Wang, X., Xia, Q., Duong, D.M., Street, C., et al. (2013). U1 small nuclear ribonucleoprotein complex and RNA splicing alterations in Alzheimer's disease. *Proc. Natl. Acad. Sci. USA* 110, 16562–16567. <https://doi.org/10.1073/pnas.1310249110>.
- Raj, T., Ryan, K.J., Replogle, J.M., Chibnik, L.B., Rosenkrantz, L., Tang, A., Rothamel, K., Stranger, B.E., Bennett, D.A., Evans, D.A., et al. (2014). CD33: increased inclusion of exon 2 implicates the Ig V-set domain in Alzheimer's disease susceptibility. *Hum. Mol. Genet.* 23, 2729–2736. <https://doi.org/10.1093/hmg/ddt666>.
- Trabzuni, D., Wray, S., Vandrovca, J., Ramasamy, A., Walker, R., Smith, C., Luk, C., Gibbs, J.R., Dillman, A., Hernandez, D.G., et al. (2012). MAPT expression and splicing is differentially regulated by brain region: relation to genotype and implication for tauopathies. *Hum. Mol. Genet.* 21, 4094–4103. <https://doi.org/10.1093/hmg/dds238>.
- Takata, A., Ionita-Laza, I., Gogos, J.A., Xu, B., and Karayiorgou, M. (2016). De Novo Synonymous Mutations in Regulatory Elements Contribute to the Genetic Etiology of Autism and Schizophrenia. *Neuron* 89, 940–947. <https://doi.org/10.1016/j.neuron.2016.02.024>.
- Quesnel-Vallières, M., Weatheritt, R.J., Cordes, S.P., and Blencowe, B.J. (2019). Autism spectrum disorder: insights into convergent mechanisms from transcriptomics. *Nat. Rev. Genet.* 20, 51–63. <https://doi.org/10.1038/s41576-018-0066-2>.
- Jaffe, A.E., Straub, R.E., Shin, J.H., Tao, R., Gao, Y., Collado-Torres, L., Kam-Thong, T., Xi, H.S., Quan, J., Chen, Q., et al. (2018). Developmental and genetic regulation of the human cortex transcriptome illuminate schizophrenia pathogenesis. *Nat. Neurosci.* 21, 1117–1125. <https://doi.org/10.1038/s41593-018-0197-y>.
- GTEX Consortium (2015). Human genomics. The Genotype-Tissue Expression (GTEx) pilot analysis: multitissue gene regulation in humans. *Science* 348, 648–660. <https://doi.org/10.1126/science.1262110>.
- Irimia, M., Weatheritt, R.J., Ellis, J.D., Parikshak, N.N., Gonatopoulos-Pournatzis, T., Babor, M., Quesnel-Vallières, M., Tapial, J., Raj, B., O'Hanlon, D., et al. (2014). A highly conserved program of neuronal microexons is misregulated in autistic brains. *Cell* 159, 1511–1523. <https://doi.org/10.1016/j.cell.2014.11.035>.
- Takata, A., Matsumoto, N., and Kato, T. (2017). Genome-wide identification of splicing QTLs in the human brain and their enrichment among schizophrenia-associated loci. *Nat. Commun.* 8, 14519. <https://doi.org/10.1038/ncomms14519>.
- Walker, R.L., Ramasamy, G., Hartl, C., Mancuso, N., Gandal, M.J., de la Torre-Ubieta, L., Pasiunic, B., Stein, J.L., and Geschwind, D.H. (2019). Genetic Control of Expression and Splicing in Developing Human Brain Informs Disease Mechanisms. *Cell* 179, 750–771.e22. <https://doi.org/10.1016/j.cell.2019.09.021>.
- Zhang, Y., Yang, H.T., Kadesh-Edmondson, K., Pan, Y., Pan, Z., Davidson, B.L., and Xing, Y. (2020). Regional Variation of Splicing QTLs in Human Brain. *Am. J. Hum. Genet.* 107, 196–210. <https://doi.org/10.1016/j.ajhg.2020.06.002>.
- Fromer, M., Roussos, P., Sieberts, S.K., Johnson, J.S., Kavanagh, D.H., Perumal, T.M., Ruderfer, D.M., Oh, E.C., Topol, A., Shah, H.R., et al. (2016). Gene expression elucidates functional impact of polygenic risk for schizophrenia. *Nat. Neurosci.* 19, 1442–1453. <https://doi.org/10.1038/nn.4399>.
- Gandal, M.J., Zhang, P., Hadjimihael, E., Walker, R.L., Chen, C., Liu, S., Won, H., van Bakel, H., Varghese, M., Wang, Y., et al. (2018). Transcriptome-wide isoform-level dysregulation in ASD, schizophrenia, and bipolar disorder. *Science* 362, eaat8127. <https://doi.org/10.1126/science.aat8127>.
- Collado-Torres, L., Burke, E.E., Peterson, A., Shin, J., Straub, R.E., Rajpurohit, A., Semick, S.A., Ulrich, W.S.; BrainSeq Consortium, and Price, A.J., et al. (2019). Regional Heterogeneity in Gene Expression, Regulation, and Coherence in the Frontal Cortex and Hippocampus across Development and Schizophrenia. *Neuron* 103, 203–216.e8. <https://doi.org/10.1016/j.neuron.2019.05.013>.
- Park, E., Pan, Z., Zhang, Z., Lin, L., and Xing, Y. (2018). The Expanding Landscape of Alternative Splicing Variation in Human Populations. *Am. J. Hum. Genet.* 102, 11–26. <https://doi.org/10.1016/j.ajhg.2017.11.002>.
- Xiong, H.Y., Alipanahi, B., Lee, L.J., Bretschneider, H., Merico, D., Yuen, R.K.C., Hua, Y., Gueroussov, S., Najafabadi, H.S., Hughes, T.R., et al. (2015). RNA splicing. The human splicing code reveals new insights into the genetic determinants of disease. *Science* 347, 1254806. <https://doi.org/10.1126/science.1254806>.
- Jin, Y., Zhang, B., Lu, J., Song, Y., Wang, W., Zhang, W., Shao, F., Gong, M., Wang, M., Liang, X., et al. (2021). Long noncoding RNA PM maintains cerebellar synaptic integrity and Cbln1 activation via Pax6/Mll1-mediated H3K4me3. *PLoS Biol.* 19, e3001297. <https://doi.org/10.1371/journal.pbio.3001297>.
- Xiao, N., Laha, S., Das, S.P., Morlock, K., Jesneck, J.L., and Raffel, G.D. (2015). Ott1 (Rbm15) regulates thrombopoietin response in hematopoietic stem cells through alternative splicing of c-Mpl. *Blood* 125, 941–948. <https://doi.org/10.1182/blood-2014-08-593392>.
- Sims, R.J., 3rd, Millhouse, S., Chen, C.F., Lewis, B.A., Erdjument-Bromage, H., Tempst, P., Manley, J.L., and Reinberg, D. (2007). Recognition of trimethylated histone H3 lysine 4 facilitates the recruitment of transcription postinitiation factors and pre-mRNA splicing. *Mol. Cell* 28, 665–676. <https://doi.org/10.1016/j.molcel.2007.11.010>.
- Wu, Y., Zeng, J., Zhang, F., Zhu, Z., Qi, T., Zheng, Y., Lloyd-Jones, L.R., Marioni, R.E., Martin, N.G., Montgomery, G.W., et al. (2018). Integrative analysis of omics summary data reveals putative mechanisms underlying complex traits. *Nat. Commun.* 9, 918. <https://doi.org/10.1038/s41467-018-03371-0>.
- Corallo, D., Donadon, M., Pantile, M., Sidorovich, V., Cocchi, S., Ori, M., De Sarlo, M., Candiani, S., Frasson, C., Distel, M., et al. (2020). LIN28B increases neural crest cell migration and leads to transformation of trunk sympathoadrenal precursors. *Cell Death Differ.* 27, 1225–1242. <https://doi.org/10.1038/s41418-019-0425-3>.
- Liang, B., Thapa, R., Zhang, G., Moffitt, C., Zhang, Y., Zhang, L., Johnston, A., Ruby, H.P., Barbera, G., Wong, P.C., et al. (2022). Aberrant neural activity in prefrontal pyramidal neurons lacking TDP-43 precedes neuron loss. *Prog. Neurobiol.* 215, 102297. <https://doi.org/10.1016/j.pneurobio.2022.102297>.
- Yang, F., Diao, X., Wang, F., Wang, Q., Sun, J., Zhou, Y., and Xie, J. (2020). Identification of Key Regulatory Genes and Pathways in Prefrontal Cortex of Alzheimer's Disease. *Interdiscip. Sci.* 12, 90–98. <https://doi.org/10.1007/s12539-019-00353-8>.
- Lennox, A.L., Hoyer, M.L., Jiang, R., Johnson-Kerner, B.L., Suit, L.A., Venkataramanan, S.,

- Sheehan, C.J., Alsina, F.C., Fregeau, B., Aldinger, K.A., et al. (2020). Pathogenic DDX3X Mutations Impair RNA Metabolism and Neurogenesis during Fetal Cortical Development. *Neuron* 106, 404–420.e8. <https://doi.org/10.1016/j.neuron.2020.01.042>.
36. Glass, J.D., Dewan, R., Ding, J., Gibbs, J.R., Dalgard, C., Keagle, P.J., Shankaracharya, García-Redondo, A., Traynor, B.J., Chia, R., and Landers, J.E. (2022). ATXN2 intermediate expansions in amyotrophic lateral sclerosis. *Brain* 145, 2671–2676. <https://doi.org/10.1093/brain/awac167>.
37. Batiuk, M.Y., Martirosyan, A., Wahis, J., de Vin, F., Marneffe, C., Kusserow, C., Koeppen, J., Viana, J.F., Oliveira, J.F., Voet, T., et al. (2020). Identification of region-specific astrocyte subtypes at single cell resolution. *Nat. Commun.* 11, 1220. <https://doi.org/10.1038/s41467-019-14198-8>.
38. Matias, I., Morgado, J., and Gomes, F.C.A. (2019). Astrocyte Heterogeneity: Impact to Brain Aging and Disease. *Front. Aging Neurosci.* 11, 59. <https://doi.org/10.3389/fnagi.2019.00059>.
39. Habib, N., McCabe, C., Medina, S., Varshavsky, M., Kitsberg, D., Dvir-Szternfeld, R., Green, G., Dionne, D., Nguyen, L., Marshall, J.L., et al. (2020). Disease-associated astrocytes in Alzheimer's disease and aging. *Nat. Neurosci.* 23, 701–706. <https://doi.org/10.1038/s41593-020-0624-8>.
40. Bulik-Sullivan, B., Finucane, H.K., Anttila, V., Gusev, A., Day, F.R., Loh, P.R.; ReproGen Consortium; Psychiatric Genomics Consortium; Genetic Consortium for Anorexia Nervosa of the Wellcome Trust Case Control Consortium 3, and Duncan, L., et al. (2015). An atlas of genetic correlations across human diseases and traits. *Nat. Genet.* 47, 1236–1241. <https://doi.org/10.1038/ng.3406>.
41. Convit, A., de Leon, M.J., Golomb, J., George, A.E., Tarshish, C.Y., Bobinski, M., Tsui, W., De Santi, S., Wegiel, J., and Wisniewski, H. (1993). Hippocampal atrophy in early Alzheimer's Disease: Anatomic specificity and validation. *Psychiatr. Q.* 64, 371–387. <https://doi.org/10.1007/BF01064929>.
42. Kulminski, A.M., Philipp, I., Shu, L., and Culminskaya, I. (2022). Definitive roles of TOMM40-APOE-APOC1 variants in the Alzheimer's risk. *Neurobiol. Aging* 110, 122–131. <https://doi.org/10.1016/j.neurobiolaging.2021.09.009>.
43. Bis, J.C., Jian, X., Kunkle, B.W., Chen, Y., Hamilton-Nelson, K.L., Bush, W.S., Salerno, W.J., Lancour, D., Ma, Y., Renton, A.E., et al. (2020). Whole exome sequencing study identifies novel rare and common Alzheimer's-Associated variants involved in immune response and transcriptional regulation. *Mol. Psychiatry* 25, 1859–1875. <https://doi.org/10.1038/s41380-018-0112-7>.
44. Tindale, L.C., Leach, S., Spinelli, J.J., and Brooks-Wilson, A.R. (2017). Lipid and Alzheimer's disease genes associated with healthy aging and longevity in healthy oldest-old. *Oncotarget* 8, 20612–20621. <https://doi.org/10.18632/oncotarget.15296>.
45. Li, J., Zhang, Y., Lu, T., Liang, R., Wu, Z., Liu, M., Qin, L., Chen, H., Yan, X., Deng, S., et al. (2022). Identification of diagnostic genes for both Alzheimer's disease and Metabolic syndrome by the machine learning algorithm. *Front. Immunol.* 13, 1037318. <https://doi.org/10.3389/fimmu.2022.1037318>.
46. Wang, Z., Zhang, Q., Lin, J.R., Jabalameli, M.R., Mitra, J., Nguyen, N., and Zhang, Z.D. (2021). Deep post-GWAS analysis identifies potential risk genes and risk variants for Alzheimer's disease, providing new insights into its disease mechanisms. *Sci. Rep.* 11, 20511. <https://doi.org/10.1038/s41598-021-99352-3>.
47. Olesen, R.H., Hyde, T.M., Kleinman, J.E., Smidt, K., Rungby, J., and Larsen, A. (2016). Obesity and age-related alterations in the gene expression of zinc-transporter proteins in the human brain. *Transl. Psychiatry* 6, e838. <https://doi.org/10.1038/tp.2016.83>.
48. Pasqualetti, G., Thayanandan, T., and Edison, P. (2022). Influence of genetic and cardiometabolic risk factors in Alzheimer's disease. *Ageing Res. Rev.* 81, 101723. <https://doi.org/10.1016/j.arr.2022.101723>.
49. Do, H., Wong, N.C., Murone, C., John, T., Solomon, B., Mitchell, P.L., and Dobrovic, A. (2014). A critical re-assessment of DNA repair gene promoter methylation in non-small cell lung carcinoma. *Sci. Rep.* 4, 4186. <https://doi.org/10.1038/srep04186>.
50. de Waard, M.C., van der Pluijm, I., Zuiderveen Borgesius, N., Comley, L.H., Haasdijk, E.D., Rijksen, Y., Ridwan, Y., Zondag, G., Hoesjmakers, J.H.J., Elgersma, Y., et al. (2010). Age-related motor neuron degeneration in DNA repair-deficient *Erc1* mice. *Acta Neuropathol.* 120, 461–475. <https://doi.org/10.1007/s00401-010-0715-9>.
51. Bennett, V., and Healy, J. (2008). Organizing the fluid membrane bilayer: diseases linked to spectrin and ankyrin. *Trends Mol. Med.* 14, 28–36. <https://doi.org/10.1016/j.molmed.2007.11.005>.
52. Iqbal, Z., Vandeweyer, G., van der Voet, M., Waryah, A.M., Zahoor, M.Y., Besseling, J.A., Roca, L.T., Vulto-van Silfhout, A.T., Nijhof, B., Kramer, J.M., et al. (2013). Homozygous and heterozygous disruptions of ANK3: at the crossroads of neurodevelopmental and psychiatric disorders. *Hum. Mol. Genet.* 22, 1960–1970. <https://doi.org/10.1093/hmg/ddt043>.
53. Morgan, A.R., Turic, D., Jehu, L., Hamilton, G., Hollingworth, P., Moskvina, V., Jones, L., Lovestone, S., Brayne, C., Rubinstztein, D.C., et al. (2007). Association studies of 23 positional/functional candidate genes on chromosome 10 in late-onset Alzheimer's disease. *Am. J. Med. Genet. Part B Neuropsychiatr. Genet.* 144B, 762–770. <https://doi.org/10.1002/ajmg.b.30509>.
54. Melé, M., Ferreira, P.G., Reverter, F., DeLuca, D.S., Monlong, J., Sammeth, M., Young, T.R., Goldmann, J.M., Pervouchine, D.D., Sullivan, T.J., et al. (2015). Human genomics. The human transcriptome across tissues and individuals. *Science* 348, 660–665. <https://doi.org/10.1126/science.1253355>.
55. Tanzi, R.E., and Bertram, L. (2001). New frontiers in Alzheimer's disease genetics. *Neuron* 32, 181–184. [https://doi.org/10.1016/S0896-6273\(01\)00476-7](https://doi.org/10.1016/S0896-6273(01)00476-7).
56. Kawles, A., Minogue, G., Zouridakis, A., Keszycki, R., Gill, N., Nassif, C., Coventry, C., Zhang, H., Rogalski, E., Flanagan, M.E., et al. (2023). Differential vulnerability of the dentate gyrus to tauopathies in dementias. *Acta Neuropathol. Commun.* 11, 1. <https://doi.org/10.1186/s40478-022-01485-7>.
57. Seo, H.J., Park, J.E., Choi, S.M., Kim, T., Cho, S.H., Lee, K.H., Song, W.K., Song, J., Jeong, H.S., Kim, D.H., and Kim, B.C. (2021). Inhibitory Neural Network's Impairments at Hippocampal CA1 LTP in an Aged Transgenic Mouse Model of Alzheimer's Disease. *Int. J. Mol. Sci.* 22, 698. <https://doi.org/10.3390/ijms22020698>.
58. Perlewitz, A., Nafz, B., Skalweit, A., Fählng, M., Persson, P.B., and Thiele, B.J. (2010). Aldosterone and vasopressin affect alpha- and gamma-EnaC mRNA translation. *Nucleic Acids Res.* 38, 5746–5760. <https://doi.org/10.1093/nar/gkq267>.
59. Khalid, Z., and Almaghrabi, O. (2020). Mutational analysis on predicting the impact of high-risk SNPs in human secretory phospholipase A2 receptor (PLA2R1). *Sci. Rep.* 10, 11750. <https://doi.org/10.1038/s41598-020-68696-7>.
60. Trubetskoy, V., Pardiñas, A.F., Qi, T., Panagiotaropoulou, G., Awasthi, S., Bigdeli, T.B., Bryois, J., Chen, C.Y., Dennison, C.A., Hall, L.S., et al. (2022). Mapping genomic loci implicates genes and synaptic biology in schizophrenia. *Nature* 604, 502–508. <https://doi.org/10.1038/s41586-022-04434-5>.
61. Mullins, N., Forstner, A.J., O'Connell, K.S., Coombes, B., Coleman, J.R.I., Qiao, Z., Als, T.D., Bigdeli, T.B., Børte, S., Bryois, J., et al. (2021). Genome-wide association study of more than 40,000 bipolar disorder cases provides new insights into the underlying biology. *Nat. Genet.* 53, 817–829. <https://doi.org/10.1038/s41588-021-00857-4>.
62. Howard, D.M., Adams, M.J., Clarke, T.K., Hafferty, J.D., Gibson, J., Shirali, M., Coleman, J.R.I., Hagenaars, S.P., Ward, J., Wigmore, E.M., et al. (2019). Genome-wide meta-analysis of depression identifies 102 independent variants and highlights the importance of the prefrontal brain regions. *Nat. Neurosci.* 22, 343–352. <https://doi.org/10.1038/s41593-018-0326-7>.
63. Wightman, D.P., Jansen, I.E., Savage, J.E., Shadrin, A.A., Bahrami, S., Holland, D., Rongve, A., Børte, S., Winsvold, B.S., Drange, O.K., et al. (2021). A genome-wide association study with 1,126,563 individuals identifies new risk loci for Alzheimer's disease. *Nat. Genet.* 53, 1276–1282. <https://doi.org/10.1038/s41588-021-00921-z>.
64. Demontis, D., Walters, G.B., Athanasiadis, G., Walters, R., Therrien, K., Nielsen, T.T., Farajzadeh, L., Voloudakis, G., Bendl, J., Zeng, B., et al. (2023). Genome-wide analyses of ADHD identify 27 risk loci, refine the genetic architecture and implicate several cognitive domains. *Nat. Genet.* 55, 198–208. <https://doi.org/10.1038/s41588-022-01285-8>.
65. van Rheenen, W., van der Spek, Bakker, M.K., van Vugt, J., Hop, P.J., Zwamborn, R.A.J., de Klein, N., Westra, H.J., Bakker, O.B., Deelen, P., et al. (2021). Common and rare variant association analyses in amyotrophic lateral sclerosis identify 15 risk loci with distinct genetic architectures and neuron-specific biology. *Nat. Genet.* 53, 1636–1648. <https://doi.org/10.1038/s41588-021-00973-1>.
66. Jiang, L., Zheng, Z., Fang, H., and Yang, J. (2021). A generalized linear mixed model association tool for biobank-scale data. *Nat. Genet.* 53, 1616–1621. <https://doi.org/10.1038/s41588-021-00954-4>.
67. Van Deerlin, Sleiman, P.M., Martinez-Lage, M., Chen-Plotkin, A., Wang, L.S., Graff-Radford, N.R., Dickson, D.W., Rademakers, R., Boeve, B.F., Grossman, M., et al. (2010). Common variants at 7p21 are associated with frontotemporal lobar degeneration with TDP-43 inclusions. *Nat. Genet.* 42, 234–239. <https://doi.org/10.1038/ng.536>.
68. Grove, J., Ripke, S., Als, T.D., Mattheisen, M., Walters, R.K., Won, H., Pallesen, J., Agerbo,

- E., Andreassen, O.A., Anney, R., et al. (2019). Identification of common genetic risk variants for autism spectrum disorder. *Nat. Genet.* 51, 431–444. <https://doi.org/10.1038/s41588-019-0344-8>.
69. Yu, G., Wang, L.G., Han, Y., and He, Q.Y. (2012). clusterProfiler: an R package for comparing biological themes among gene clusters. *OMICS A J. Integr. Biol.* 16, 284–287. <https://doi.org/10.1089/omi.2011.0118>.
70. Chen, S., Zhou, Y., Chen, Y., and Gu, J. (2018). fastp: an ultra-fast all-in-one FASTQ preprocessor. *Bioinformatics* 34, i884–i890. <https://doi.org/10.1093/bioinformatics/bty560>.
71. Dobin, A., Davis, C.A., Schlesinger, F., Drenkow, J., Zaleski, C., Jha, S., Batut, P., Chaisson, M., and Gingeras, T.R. (2013). STAR: ultrafast universal RNA-seq aligner. *Bioinformatics* 29, 15–21. <https://doi.org/10.1093/bioinformatics/bts635>.
72. van de Geijn, B., McVicker, G., Gilad, Y., and Pritchard, J.K. (2015). WASP: allele-specific software for robust molecular quantitative trait locus discovery. *Nat. Methods* 12, 1061–1063. <https://doi.org/10.1038/nmeth.3582>.
73. Li, Y.I., Knowles, D.A., Humphrey, J., Barbeira, A.N., Dickinson, S.P., Im, H.K., and Pritchard, J.K. (2018). Annotation-free quantification of RNA splicing using LeafCutter. *Nat. Genet.* 50, 151–158. <https://doi.org/10.1038/s41588-017-0004-9>.
74. Ongen, H., Buil, A., Brown, A.A., Dermitzakis, E.T., and Delaneau, O. (2016). Fast and efficient QTL mapper for thousands of molecular phenotypes. *Bioinformatics* 32, 1479–1485. <https://doi.org/10.1093/bioinformatics/btv722>.
75. Quinlan, A.R., and Hall, I.M. (2010). BEDTools: a flexible suite of utilities for comparing genomic features. *Bioinformatics* 26, 841–842. <https://doi.org/10.1093/bioinformatics/btq033>.
76. Purcell, S., Neale, B., Todd-Brown, K., Thomas, L., Ferreira, M.A.R., Bender, D., Maller, J., Sklar, P., de Bakker, P.I.W., Daly, M.J., and Sham, P.C. (2007). PLINK: a tool set for whole-genome association and population-based linkage analyses. *Am. J. Hum. Genet.* 81, 559–575. <https://doi.org/10.1086/519795>.
77. Zhang, B., and Horvath, S. (2005). A general framework for weighted gene co-expression network analysis. *Stat. Appl. Genet. Mol. Biol.* 4, Article17. <https://doi.org/10.2202/1544-6115.1128>.
78. Gusev, A., Ko, A., Shi, H., Bhatia, G., Chung, W., Penninx, B.W.J.H., Jansen, R., de Geus, E.J.C., Boomsma, D.I., Wright, F.A., et al. (2016). Integrative approaches for large-scale transcriptome-wide association studies. *Nat. Genet.* 48, 245–252. <https://doi.org/10.1038/ng.3506>.
79. Skene, N.G., and Grant, S.G.N. (2016). Identification of Vulnerable Cell Types in Major Brain Disorders Using Single Cell Transcriptomes and Expression Weighted Cell Type Enrichment. *Front. Neurosci.* 10, 16. <https://doi.org/10.3389/fnins.2016.00016>.
80. Cingolani, P., Platts, A., Wang, L.L., Coon, M., Nguyen, T., Wang, L., Land, S.J., Lu, X., and Ruden, D.M. (2012). A program for annotating and predicting the effects of single nucleotide polymorphisms, SnpEff: SNPs in the genome of *Drosophila melanogaster* strain w1118; iso-2; iso-3. *Fly* 6, 80–92. <https://doi.org/10.4161/fly.19695>.
81. Yang, J., Lee, S.H., Goddard, M.E., and Visscher, P.M. (2011). GCTA: a tool for genome-wide complex trait analysis. *Am. J. Hum. Genet.* 88, 76–82. <https://doi.org/10.1016/j.ajhg.2010.11.011>.
82. 1000 Genomes Project Consortium, Abecasis, G.R., Auton, A., Brooks, L.D., DePristo, M.A., Durbin, R.M., Handsaker, R.E., Kang, H.M., Marth, G.T., and McVean, G.A. (2012). An integrated map of genetic variation from 1,092 human genomes. *Nature* 491, 56–65. <https://doi.org/10.1038/nature11632>.
83. McLaren, W., Pritchard, B., Rios, D., Chen, Y., Flicek, P., and Cunningham, F. (2010). Deriving the consequences of genomic variants with the Ensembl API and SNP Effect Predictor. *Bioinformatics* 26, 2069–2070. <https://doi.org/10.1093/bioinformatics/btq330>.
84. ENCODE Project Consortium (2012). An integrated encyclopedia of DNA elements in the human genome. *Nature* 489, 57–74. <https://doi.org/10.1038/nature11247>.
85. Mei, S., Qin, Q., Wu, Q., Sun, H., Zheng, R., Zang, C., Zhu, M., Wu, J., Shi, X., Taing, L., et al. (2017). Cistrome Data Browser: a data portal for ChIP-Seq and chromatin accessibility data in human and mouse. *Nucleic Acids Res.* 45, D658–d662. <https://doi.org/10.1093/nar/gkw983>.
86. Boyle, A.P., Hong, E.L., Hariharan, M., Cheng, Y., Schaub, M.A., Kasowski, M., Karczewski, K.J., Park, J., Hitz, B.C., Weng, S., et al. (2012). Annotation of functional variation in personal genomes using RegulomeDB. *Genome Res.* 22, 1790–1797. <https://doi.org/10.1101/gr.137323.112>.
87. Yang, Y.C.T., Di, C., Hu, B., Zhou, M., Liu, Y., Song, N., Li, Y., Umetsu, J., and Lu, Z.J. (2015). CLIPdb: a CLIP-seq database for protein-RNA interactions. *BMC Genom.* 16, 51. <https://doi.org/10.1186/s12864-015-1273-2>.
88. Kuhn, R.M., Haussler, D., and Kent, W.J. (2013). The UCSC genome browser and associated tools. *Brief. Bioinform.* 14, 144–161. <https://doi.org/10.1093/bib/bbs038>.
89. Welter, D., MacArthur, J., Morales, J., Burdett, T., Hall, P., Junkins, H., Klemm, A., Flicek, P., Manolio, T., Hindorf, L., and Parkinson, H. (2014). The NHGRI GWAS Catalog, a curated resource of SNP-trait associations. *Nucleic Acids Res.* 42, D1001–D1006. <https://doi.org/10.1093/nar/gkt1229>.
90. Finucane, H.K., Bulik-Sullivan, B., Gusev, A., Trynka, G., Reshef, Y., Loh, P.R., Anttila, V., Xu, H., Zang, C., Farh, K., et al. (2015). Partitioning heritability by functional annotation using genome-wide association summary statistics. *Nat. Genet.* 47, 1228–1235. <https://doi.org/10.1038/ng.3404>.
91. Bulik-Sullivan, B.K., Loh, P.R., Finucane, H.K., Ripke, S., Yang, J., Schizophrenia Working Group of the Psychiatric Genomics Consortium, Patterson, N., Daly, M.J., Price, A.L., and Neale, B.M. (2015). LD Score regression distinguishes confounding from polygenicity in genome-wide association studies. *Nat. Genet.* 47, 291–295. <https://doi.org/10.1038/ng.3211>.
92. International HapMap Consortium (2003). The International HapMap Project. *Nature* 426, 789–796. <https://doi.org/10.1038/nature02168>.
93. 1000 Genomes Project Consortium, Auton, A., Brooks, L.D., Durbin, R.M., Garrison, E.P., Kang, H.M., Korbel, J.O., Marchini, J.L., McCarthy, S., McVean, G.A., and Abecasis, G.R. (2015). A global reference for human genetic variation. *Nature* 526, 68–74. <https://doi.org/10.1038/nature15393>.
94. Zeisel, A., Muñoz-Manchado, A.B., Codeluppi, S., Lönnerberg, P., La Manno, G., Juréus, A., Marques, S., Munguba, H., He, L., Betsholtz, C., et al. (2015). Brain structure. Cell types in the mouse cortex and hippocampus revealed by single-cell RNA-seq. *Science* 347, 1138–1142. <https://doi.org/10.1126/science.aaa1934>.
95. Frankish, A., Diekhans, M., Ferreira, A.M., Johnson, R., Jungreis, I., Loveland, J., Mudge, J.M., Sisu, C., Wright, J., Armstrong, J., et al. (2019). GENCODE reference annotation for the human and mouse genomes. *Nucleic Acids Res.* 47, D766–d773. <https://doi.org/10.1093/nar/gky955>.
96. Li, X., Su, X., Liu, J., Li, H., Li, M., 23andMe Research Team, Li, W., and Luo, X.J. (2021). Transcriptome-wide association study identifies new susceptibility genes and pathways for depression. *Transl. Psychiatry* 11, 306. <https://doi.org/10.1038/s41398-021-01411-w>.

STAR★METHODS

KEY RESOURCES TABLE

REAGENT or RESOURCE	SOURCE	IDENTIFIER
Deposited data		
GWAS of SCZ	Trubetsky et al. ⁶⁰	https://pgc.unc.edu/for-researchers/download-results/
GWAS of BP	Mullins et al. ⁶¹	https://pgc.unc.edu/for-researchers/download-results/
GWAS of DEP	Howard et al. ⁶²	https://pgc.unc.edu/for-researchers/download-results/
GWAS of ALZ	Douglas et al. ⁶³	https://pgc.unc.edu/for-researchers/download-results/
GWAS of ADHD	Demontis et al. ⁶⁴	https://pgc.unc.edu/for-researchers/download-results/
GWAS of ALS	Wouter et al. ⁶⁵	https://www.ebi.ac.uk/gwas/efotraits/MONDO_0004976
GWAS of PD	Jiang L et al. ⁶⁶	https://www.ebi.ac.uk/gwas/efotraits/MONDO_0005180
GWAS of MS	Jiang L et al. ⁶⁶	https://www.ebi.ac.uk/gwas/efotraits/MONDO_0005301
GWAS of FTD	Deerlin et al. ⁶⁷	https://gwas.mrcieu.ac.uk/datasets/ieu-b-43/
GWAS of Stroke	Jiang L et al. ⁶⁶	https://www.ebi.ac.uk/gwas/efotraits/EFO_0000712
GWAS of Autism	Jakob et al. ⁶⁸	https://pgc.unc.edu/for-researchers/download-results/
GWAS of Epilepsy	Jiang L et al. ⁶⁶	https://www.ebi.ac.uk/gwas/efotraits/EFO_0000474
Software and algorithms		
R softwares	R project	https://www.r-project.org/
clusterProfiler R package	Yu et al. ⁶⁹	https://mrcieu.github.io/TwoSampleMR
fastp	Chen et al. ⁷⁰	https://github.com/OpenGene/fastp
STAR	Dobin et al. ⁷¹	https://github.com/alexdobin/STAR
WASP	van de Geijn et al. ⁷²	https://github.com/bmvdgeijn/WASP
LeafCutter	Li et al. ⁷³	https://github.com/davidaknowles/leafcutter
FastQTL	Halit et al. ⁷⁴	https://github.com/francois-a/fastqtl
BEDtools	Quinlan et al. ⁷⁵	https://github.com/arq5x/bedtools2
PLINK1.9	Purcell et al. ⁷⁶	https://www.cog-genomics.org/plink/1.9/
LDSC	Bulik et al. ⁴⁰	https://github.com/bulik/ldsc
WGCNA R package	Peter et al. ⁷⁷	http://www.genetics.ucla.edu/labs/horvath/CoexpressionNetwork/Rpackages/WGCNA
FUSION	Gusev et al. ⁷⁸	https://github.com/gusevlab/fusion_twos
EWCE	Nathan et al. ⁷⁹	https://github.com/NathanSkene/EWCE
SnEff	Pablo et al. ⁸⁰	https://pcingola.github.io/SnpEff/

RESOURCE AVAILABILITY

Lead contact

Further information and requests for resources and reagents should be directed to and will be fulfilled by the lead contact: Prof, Junfeng Xia (jfxia@ahu.edu.cn).

Materials availability

This study did not generate new unique reagents.

Data and code availability

- This paper does not report original code.
- Data reported in this paper will be shared by the [lead contact](#) upon request. Any additional information required to reanalyze the data reported in this paper is available from the corresponding author upon reasonable request.

METHOD DETAILS

RNA-seq data of the HIPPO tissue

The RNA-seq FASTQ files for the HIPPO region of human brain were downloaded from BrainSeq2²⁵ database (<http://eqtl.brainseq.org/phase2/>) via Globus file transfer tool. Participants with no prior history of neurological and/or neuropsychiatric conditions were included in the study, and the final number of individuals included in this study was N = 264 (The detailed ancestry distribution is shown in [Figure S1](#)). Briefly, total RNA was extracted by using RNeasy Lipid Tissue Mini Kit (QIAGEN). Paired-end sequencing libraries preparation was performed using the TruSeq Stranded Total RNA Library kit (Illumina), after which the libraries were sequenced using Illumina HiSeq 3000 platform. The procedures for sample preparation, RNA sequencing, quality check and data processing have been described in detail in the original study.²⁵ Downloaded FASTQ files for mapped reads from each individual were pre-processed for quality control with fastp⁷⁰ and then converted into BAM files by using STAR.⁷¹

SNP genotyping data

Additional quality-controlled DNA genotyping data for the same HIPPO individuals (N = 264) were also obtained from the BrainSeq2 resource dataset. The genotyping of DNA samples was performed on the Illumina platform (build hg19/GRCh37). The human postmortem brain tissue was obtained by autopsy primarily from the Offices of the Chief Medical Examiner of the District of Columbia, and the National Institute of Child Health and Human Development Brain and Tissue Bank for Developmental Disorders. After imputation and quality control (SNPs with MAF >5% and Hardy-Weinberg $p > 1 \times 10^{-6}$) steps, totaling 7,023,860 high-quality variants remained in this dataset. More detailed information about quality assessment, genotyping analysis, and SNPs identification can be found in the originally literature.²⁵ Of these remaining SNPs, we extracted all SNPs that are within ± 100 kb of the identified AS events and used them for *cis*-sQTL mapping.

Detection and quantification of AS events

To comprehensively perform splicing analyses of RNA-seq data from HIPPO tissue, we used the LeafCutter algorithm⁷³ to calculate intron excision ratios, which represents the proportion of usage of an intron relative to other introns in the same cluster. The 'percentage spliced-in' value (PSI) was calculated as a quantification of the intron excision. Before running LeafCutter, the alignment and quantification of RNA-seq reads (i.e., converted BAM files) were processed using STAR⁷¹ and reads exhibiting potential mapping bias were removed with WASP.⁷² We then ran LeafCutter with default parameter settings to perform intron clustering, which allows maximum introns with length up to 500 kb. By using `prepare_genotype_table.py` script in LeafCutter, intron excision ratios were calculated and introns used in less than 40% of individuals or with almost no variation were filtered out. After normalization and quantile standardization of intron excision rates, the final splicing expression matrix (i.e., PSI matrix) was obtained, which could be used as the standard input data for FastQTL.⁷⁴

Splicing QTL mapping

To explore significant associations between SNP dosages and PSI of AS, we performed *cis*-sQTL mapping (within 100 kb of intron clusters) using linear regression implemented in the FastQTL software.⁷⁴ Considering the influence of genetic, biological, and technical factors, we conducted covariance correction analysis to control potential confounding variables. For the selection of covariates, we first employed the first five principal components derived using GCTA⁸¹ of the genotype matrix to account for the influence of genetic ancestry, as well as the first 10 principal components of the PSI phenotype matrix to regress out the effect of known/hidden factors. The principal components analysis was then conducted to regress out the technical and biological covariates such as age, sex and RNA integrity number (RIN). Furthermore, we ran the permute comparison model in FastQTL and set 1,000–100,000 adaptive permutes to calculate the p-value (i.e., permutation p-value) for each significant sQTL SNP. The calculated Beta-approximated empirical p-values were corrected using the Benjamini-Hochberg correction to account for the multiple tests, and we detected all significant sQTLs (FDR <0.05) corresponding to AS events.

sQTL and non-sQTL datasets generating

To further characterize the sQTL SNPs, we generated two sets of sQTL and non-sQTL SNPs for comparative analysis by screening Benjamini-Hochberg corrected p -values and pruning SNPs. Specifically, we first selected the most significant SNP (i.e., the most representative sQTL SNP for each AS event) among the sQTL SNPs after correcting the p values. And the SNPs screened above with linkage disequilibrium (LD) were pruned using PLINK software (version 1.9)⁷⁶ with the parameters “-indep-pairwise 50 5 0.5”, which represent window size, shift step and r^2 threshold, respectively. The haplotype of 1000 Genome Project Phase 3 (EUR)⁸² were used as the reference genotypes for LD-based pruning in PLINK. For the dataset of sQTL SNPs, we extracted a total of 6,966 SNPs that contributed to AS regulation independently of each other after screening the most significant SNPs among the sQTL SNPs with corrected p value <0.05 and LD pruning. For the controlled dataset of non-sQTL SNPs, we obtained a total of 124,801 SNPs that did not contribute to AS regulation and independent of one another through screening the most significant SNPs among the sQTL SNPs with uncorrected p value >0.05 , and LD pruning with the same setting. Overall, we generated 6,966 sQTL SNPs and 124,801 non-sQTL SNPs strongly independent of each other for downstream analysis, including functional annotation and functional enrichment analysis.

Functional annotation of sQTL and non-sQTL SNPs

For sQTL and non-sQTL SNPs, we functionally annotated these SNPs using SnpEff v5.1.⁸⁰ Information on SnpEff annotations was gathered using MyVariant.info (<http://myvariant.info/>) and VeP (Variant Effect Predictor).⁸³ Based on the annotation information, the variants (including sQTL and non-sQTL SNPs) were classified into 9 categories, and overlapping functional categories were prioritized as: synonymous > 5' UTR > 3' UTR > intergenic > intron > splice region (defined as the variant within 1–3 bases of exon and 3–8 bases of intron from the nearest intron–exon boundary) > non-coding exon > splice acceptor > splice donor. Based on the different functional classifications of sQTL SNPs, we then performed enrichment analysis for each functional class of sQTL SNPs using Fisher's exact test for 2×2 table (i.e., the rows listed as SNPs "belonged" and "not belonged" to the specific classification, and columns listed as sQTL SNPs and non-sQTL SNPs).

Functional enrichment of sQTL SNPs among genetic regulatory elements and splicing factor binding sites

To investigate the functional enrichment of sQTL SNPs in various regulatory elements in HIPPO tissue, we downloaded the histones annotation information with BED format (including monomethylated histone H3 lysine 4 (H3K4me1), trimethylated histone H3 lysine 4 (H3K4me3), acetylated histone H3 lysine 9 (H3K9ac), acetylated histone H3 lysine 27 (H3K27ac) and DNase I hypersensitive sites (DHS)) from the Encyclopedia of DNA Elements project (ENCODE portal⁸⁴) and CistromeDB⁸⁵ database. BEDTools⁷⁵ was used to analyze whether SNPs are included in these regulatory elements. In addition to the histones, transcription factor (TF) is another important transcriptional regulator involved in transcriptional regulation. To determine the effect of SNPs on gene transcriptional regulation by TF, we scored these variants using RegulomeDB⁸⁶ v2.0 (<http://www.regulomedb.org>), which allowed us to focus on non-coding variants that may directly affect TF binding (i.e., categories 1 and 2 defined by RegulomeDB).

Considering that AS events are largely regulated by RNA binding proteins (RBP), we also downloaded publicly available human RBP binding sites data (bed format files and built hg38) from CLIPdb database.⁸⁷ We utilized liftOver⁸⁸ to convert the coordinates of sQTL SNPs from hg19 to hg38 and used BEDTools to assess the enrichment of sQTL SNPs on RBP binding site. Ultimately, the enrichment analyses of sQTL SNPs among genetic regulatory elements and RBP binding sites were conducted by Fisher's exact test with 2×2 table (i.e., the rows listed as SNPs within and not within the regulatory element and RBP binding sites, and columns listed as sQTL SNPs and non-sQTL SNPs).

Functional enrichment of sQTLs among brain disease-associated loci

SNPs in high LD with the sQTL SNPs ($r^2 > 0.8$) were calculated with PLINK software using the 1000 Genomes Project reference data. We downloaded GWAS variants information from the GWAS Catalog v.1.0.2⁸⁹ (only SNPs with P values $< 1 \times 10^{-5}$ were included in this list) and then used these GWAS variants information to annotate high LD SNPs. BEDTools was used to determine whether the SNPs obtained above falls within disease-associated loci. Moreover, we performed functional enrichment analysis of sQTLs among brain disease-associated loci by Fisher's exact test with 2×2 table (i.e., the rows listed as SNPs within and not within the brain disease-associated loci, and columns listed as sQTL SNPs and non-sQTL SNPs). We conducted enrichment analyses for the following 12 brain disorders: Alzheimer, amyotrophic lateral sclerosis, Parkinson, frontotemporal dementia, epilepsy, autism, schizophrenia, bipolar disorder, depression, attention deficit hyperactivity disorder, multiple sclerosis, and stroke.

DLPFC and HIPPO tissue comparison

To compare effect sizes consistently between DPPFC and HIPPO brain regions, we also obtained RNA-seq data in the BrainSeq2 for DLPFC with the same samples as HIPPO, and the related data processing can be found in the original publication.²⁵ The RNA-seq data processing procedure (including quality control, PSI calculating and sQTL detecting) of DLPFC is the same as that of HIPPO. For SNPs corresponding to multiple splicing events at a single mutation site, we selected the SNP with the smallest P value. Eventually, we identified 8,423 sQTL SNPs in DLPFC for subsequent comparative analysis, including partitioned heritability.

Partitioned heritability

LD Score software v1.0.1^{90,91} was used to calculate partitioned heritability to identify enrichment of GWAS summary statistics in DLPFC and HIPPO brain regions. The sQTL annotations from both brain regions were created by using a window size of 500 bp (± 250 bp) around each sQTL SNPs, resulting in 11,157 HIPPO sQTL annotations (Table S1) and 13,383 DLPFC sQTL annotations (Table S2). The annotation files were created by tagging all HapMap3⁹² SNPs that fell within the sQTL annotations. By using 1000 Genomes Phase 3 (EUR)⁹³ as LD reference panel, we calculated LD-scores with an LD window of 1 cM. The enrichment of each annotation was calculated by dividing the proportion of heritability explained by each annotation by the proportion of SNPs in the genome that fell into that annotation category. The sQTLs in DLPFC and HIPPO tissue were examined separately for enrichment in genetic variants associated with 12 brain disorders mentioned in Section [functional enrichment of sQTLs among brain disease-associated loci](#).

Expression-weighted cell type enrichment analysis (EWCE)

To explore sQTLs-relevant cell types, we employed R package to perform cell type enrichment analysis for sQTL SNPs sets. We downloaded single-cell RNA-seq gene expression data of mouse somatosensory cortex and hippocampal CA1 region from Zeisel et al.,⁹⁴ including 9 cell types and 47 cell subclasses. The EWCE R-package⁷⁹ was used to investigate cell-type expression specificity of identified sQTL-related genes, and analysis results were considered to be significant at $P < 0.05$. Further details on the principles, model algorithm implementation of the EWCE analysis can be found in the publication.⁷⁹

Weighted gene co-expression network analysis (WGCNA)

We mapped intron clusters (obtained from the LeafCutter) to sGenes based on the hg19 reference genome annotation downloaded from GENCODE.⁹⁵ The individual genes corresponding to multiple probe sets were merged, resulting in a final splicing matrix of 15,277 genes. Network analysis was performed by a robust consensus WGCNA (rWGCNA)⁷⁷ to cluster sGenes into specific modules based on biased intermediate correlations among gene expression patterns. A soft-threshold power of 5 was chosen to achieve approximate scale-free topology of the network ($r^2 > 0.9$), and each co-expression network used the same estimated power parameter. Gene modules were defined by using the topological overlap dendrogram with specific module cutting parameters (deepSplit = 2, minimum module size = 30, merge threshold = 0.25), and sex and age were selected as phenotypes. For each module of genes, we performed Gene Ontology (GO) and Kyoto Encyclopedia of Genes and Genomes (KEGG) pathway enrichment analysis using the clusterProfiler R package.⁶⁹ The calculated P values were corrected with Benjamini-Hochberg correction and top two significant terms are reported.

TWAS analysis

We performed TWAS analysis using the FUSION package (<http://gusevlab.org/projects/fusion/>) by integrating GWAS summary statistics of Alzheimers disease⁶³ and PSI in HIPPO brain tissue. The SNP-based predictive weights of each intron in HIPPO were calculated by the computational weight pipeline described in FUSION, which represents the correlation between SNPs and AS regulation in the reference panel. Furthermore, TWAS was performed using the FUSION software⁷⁸ with several regularized linear models (including Elastic Net, LASSO, and BLUP) to evaluate the imputation of the expressions. More details of the TWAS analysis can be found in our previous study.⁹⁶ The absolute value of the Z-score calculated by TWAS reflects the strength of the association between the intron usage (i.e., AS events) of interest and the disease. The multiple correction was applied to the TWAS analysis results, and the significance level was set at 1.13×10^{-5} (Bonferroni correction 0.05/4,420).

Multiple comparison

To avoid the false positive and false negative results, the Bonferroni correction and Benjamini-Hochberg correction for multiple testing were applied to the analysis results in our study. For all enrichment analysis and TWAS analysis, the P -value adjustments were performed using Bonferroni correction method. For sQTL mapping, EWCE and WGCNA analysis, the P -value was further corrected with Benjamini-Hochberg method.

QUANTIFICATION AND STATISTICAL ANALYSIS

All quantification and statistical analyses were performed as described in the [method details](#) section of the [STAR methods](#).